NASA/TM—2002-211588

Combustion Temperature Measurement by Spontaneous Raman Scattering in a Jet-A Fueled Gas Turbine Combustor Sector

Yolanda R. Hicks
Glenn Research Center, Cleveland, Ohio

Wilhelmus A. De Groot
Silicon Light Machines, Sunnyvale, California

Randy J. Locke
QSS Group, Inc., Cleveland, Ohio

Robert C. Anderson
Glenn Research Center, Cleveland, Ohio

May 2002

The NASA STI Program Office . . . in Profile

Since its founding, NASA has been dedicated to the advancement of aeronautics and space science. The NASA Scientific and Technical Information (STI) Program Office plays a key part in helping NASA maintain this important role.

The NASA STI Program Office is operated by Langley Research Center, the Lead Center for NASA's scientific and technical information. The NASA STI Program Office provides access to the NASA STI Database, the largest collection of aeronautical and space science STI in the world. The Program Office is also NASA's institutional mechanism for disseminating the results of its research and development activities. These results are published by NASA in the NASA STI Report Series, which includes the following report types:

- TECHNICAL PUBLICATION. Reports of completed research or a major significant phase of research that present the results of NASA programs and include extensive data or theoretical analysis. Includes compilations of significant scientific and technical data and information deemed to be of continuing reference value. NASA's counterpart of peer-reviewed formal professional papers but has less stringent limitations on manuscript length and extent of graphic presentations.

- TECHNICAL MEMORANDUM. Scientific and technical findings that are preliminary or of specialized interest, e.g., quick release reports, working papers, and bibliographies that contain minimal annotation. Does not contain extensive analysis.

- CONTRACTOR REPORT. Scientific and technical findings by NASA-sponsored contractors and grantees.

- CONFERENCE PUBLICATION. Collected papers from scientific and technical conferences, symposia, seminars, or other meetings sponsored or cosponsored by NASA.

- SPECIAL PUBLICATION. Scientific, technical, or historical information from NASA programs, projects, and missions, often concerned with subjects having substantial public interest.

- TECHNICAL TRANSLATION. English-language translations of foreign scientific and technical material pertinent to NASA's mission.

Specialized services that complement the STI Program Office's diverse offerings include creating custom thesauri, building customized data bases, organizing and publishing research results . . . even providing videos.

For more information about the NASA STI Program Office, see the following:

- Access the NASA STI Program Home Page at ***http://www.sti.nasa.gov***

- E-mail your question via the Internet to help@sti.nasa.gov

- Fax your question to the NASA Access Help Desk at 301–621–0134

- Telephone the NASA Access Help Desk at 301–621–0390

- Write to:
  NASA Access Help Desk
  NASA Center for AeroSpace Information
  7121 Standard Drive
  Hanover, MD 21076

NASA/TM—2002-211588

Combustion Temperature Measurement by Spontaneous Raman Scattering in a Jet-A Fueled Gas Turbine Combustor Sector

Yolanda R. Hicks
Glenn Research Center, Cleveland, Ohio

Wilhelmus A. De Groot
Silicon Light Machines, Sunnyvale, California

Randy J. Locke
QSS Group, Inc., Cleveland, Ohio

Robert C. Anderson
Glenn Research Center, Cleveland, Ohio

National Aeronautics and
Space Administration

Glenn Research Center

May 2002

Acknowledgments

We gratefully recognize and thank the crew of engineers and technicians in ASCR who supported the test and us.

This report is a formal draft or working paper, intended to solicit comments and ideas from a technical peer group.

This report contains preliminary findings, subject to revision as analysis proceeds.

Available from

NASA Center for Aerospace Information
7121 Standard Drive
Hanover, MD 21076

National Technical Information Service
5285 Port Royal Road
Springfield, VA 22100

Available electronically at http://gltrs.grc.nasa.gov/GLTRS

Combustion Temperature Measurement by Spontaneous Raman Scattering in a Jet-A Fueled Gas Turbine Combustor Sector

Yolanda R. Hicks
National Aeronautics and Space Administration
Glenn Research Center
Cleveland, Ohio 44135

Wilhelmus A. De Groot
Silicon Light Machines
Sunnyvale, California 94089

Randy J. Locke
QSS Group, Inc.
Cleveland, Ohio 44135

Robert C. Anderson
National Aeronautics and Space Administration
Glenn Research Center
Cleveland, Ohio 44135

Abstract

Spontaneous vibrational Raman scattering was used to measure temperature in an aviation combustor sector burning jet fuel. The inlet temperature ranged from 670 K (750 °F) to 756 K (900 °F) and pressures from 13 bar to 55 bar. With the exception of a discrepancy that we attribute to soot, good agreement was seen between the Raman-derived temperatures and the theoretical temperatures calculated from the inlet conditions. The technique used to obtain the temperature uses the relationship between the N_2 anti-Stokes and Stokes signals, within a given Raman spectrum. The test was performed using a NASA-concept fuel injector and Jet-A fuel over a range of fuel/air ratios. This work represents the first such measurements in a high-pressure, research aero-combustor facility.

Introduction

NASA Glenn Research Center (GRC) is working with the aeronautics industry to develop more fuel-efficient and environmentally friendly gas turbine combustor technology. This effort includes testing new hardware designs at conditions that simulate the high-temperature, high-pressure environment expected in the next-generation of high-performance engines. NASA GRC has the only high flow rate facilities that provide both high pressure and high inlet temperatures in which such tests can be performed. The GRC facilities are also unique because the combustor facilities have windows that provide the opportunity to non-intrusively interrogate the combustor flow field. Thus, a major aspect of the testing uses non-intrusive optical and laser diagnostics to determine combustion species concentration, fuel/air ratio, fuel drop size and velocity, degree of mixedness, and to visualize the fuel injector spray pattern and combustion species distributions (Hicks et al. 2000; Locke et al. 2001).

Typically, to assess its performance, a test article (the candidate fuel injector concept hardware) is installed in the facility and run through a matrix of conditions that vary the fuel and airflow rates, temperatures and pressures. A variety of measurements are taken during the tests and used to make that diagnosis. A single test article will be run through the matrix only a few times—once is quite typical when using laser diagnostics—before a new test article is installed. Given this constraint it makes sense to apply optical techniques that have been successfully used in bench top hydrocarbon flames that we feel can be implemented practically in a realistic, dirty, environment with limited optical access, where the test hardware changes frequently. A very real requirement in such an environment is to be user friendly to those responsible for test facilities and hardware on a day-to-day basis as well as to those responsible for the laser diagnostics; both groups require access to the same limited physical space.

The data we obtain using optical diagnostics are used by designers to determine the efficacy of specific designs, and also provide a database for combustion modelers, and enhance our understanding of the many processes that take place within a combustor. The ability to measure temperature is one capability that we are pursuing. This article summarizes our latest developments in the temperature measurement arena, using spontaneous Raman scattering.

Spontaneous Raman scattering allows one to measure combustion species concentration and/or temperature. A Raman measurement typically yields a spectrum the area of whose peaks are linearly related to the number density of the molecular species. Although there are many approaches, measuring temperature with vibrational Raman spectroscopy is generally conducted in one of three ways (Lederman, 1977; Eckbreth, 1988; Laurendeau, 1988). One might take advantage of the additional rotational lines that appear with increasing temperature, and determine the temperature by fitting the data to theory. Another approach is to use the total number density of the major species to derive the temperature thermodynamically. Alternately, one can compare the vibrational intensities of Stokes and anti-Stokes peaks for a particular species (Karpetis and Gomez, 1996). It is the latter method we use and report herein.

We first describe the theory of Raman scattering, emphasizing the Stokes/anti-Stokes ratio method. We then describe the experimental hardware, which includes the Advanced Subsonic Combustion Rig facility, the test article and the laser facility. We next describe our experimental procedure and test matrix. Finally, we present and discuss our results and offer suggestions for future work.

Theory

Raman Scattering

Raman scattering is a process in which there is inelastic interaction of the incident radiation with a molecular system whereby the molecules as a whole will have picked up energy or released energy as a result of the interaction; thus the incident and scattered wavelengths are not the same. Each molecular species scatters energy at different specific wavelengths that reflect the internal energy of the species, due in part to the vibrational and rotational—rovibrational—energy of the molecular bonds. In the case of Raman spectroscopy, the incident electromagnetic field (in this case, a laser beam) induces in the molecule an oscillating dipole whose strength depends on the rovibrational components of molecular energy. Because the nature of bonds in each molecular species is different, so arises a unique Raman spectrum for each species. Also, because the energy of these bonds can be different depending on the temperature and pressure, the spectra for a species may also appear different under varying conditions. Stokes lines reflect an energy exchange with the laser in which the molecules gain energy from incident laser photons. Stokes (S) lines will always be present when molecules exist in the ground and first excited vibrational states. Anti-Stokes (AS) lines appear once the Boltzmann distribution of molecules is such that some molecules in the system have higher vibrational energy, usually as a result of higher system temperature.

We derive temperature from the Raman spectra using as basis the derivation

$$T = \frac{h\nu c}{k}\left[\ln\left\{C(\nu_S, \nu_{AS})\frac{I_S}{I_{AS}}\right\} + 4\ln\left\{\frac{\nu_0 + \nu}{\nu_0 - \nu}\right\}\right]^{-1} \quad (1)$$

adapted from Lederman (1977), who provides an in-depth review of Raman spectroscopy in combustion. h and k are the Planck and Boltzmann constants, c is the speed of light, ν_0 is the laser frequency, ν is the Raman frequency shift (cm^{-1}), and $\nu_S = \nu_0 - \nu$ and $\nu_{AS} = \nu_0 + \nu$ are the stokes and anti-Stokes frequencies. The term I_S/I_{AS} is the intensity ratio of Stokes scattering to anti-Stokes scattering. The constant term $C(\nu_S, \nu_{AS})$ is the wavelength-dependent efficiency of the collection/dispersion/detection system.

Thus the temperature can be extracted when the integrated Stokes and Anti-Stokes collected energies have been measured and when the wavelength correction parameter has been established. Figure 1 plots the temperature as a function of anti-Stokes/Stokes ratio for several values of C. The constant has great influence on the slope—and therefore the sensitivity—of the AS/S ratio in determining the temperature. To determine the constant's value one typically heats nitrogen in a closely controlled test vessel, obtains spectra and determines the AS/S ratio over a range of temperature. Those ratios are compared with theory to determine the best fit.

Experimental

Combustor Facility

The Advanced Subsonics Combustor Rig (ASCR) facility's sector rig is based on a shell-in-shell concept in which the outer shell serves as the pressure vessel and inlet air plenum while the inner shell is the actual combustor hardware, equipped to withstand (we hope) the heat of combustion. This arrangement allows one to test small combustors or sectors of large combustors.

In the present case, the combustor hardware is a 15-degree combustor sector that uses a multipoint lean direct injection (LDI) concept (Tacina et al. 2002). The injector hardware is pictured in figure 2 and described by Mansour et al. (2001). Flow passes from left to right. It consists of a four-by-nine matrix of fuel/air injection points in an arc that is 15° (1/24) of a full-annular combustor. The sector walls are effusion-cooled and flame-sprayed to cool and protect them from the heat.

To provide laser and optical access, the side and top (liner) walls are replaced with walls that are equipped with windows, shown in figures 3 and 4. The ultraviolet-grade, synthetic fused silica windows are positioned so as to observe the region immediately downstream of the fuel injectors. Side windows have a clear aperture 7-cm high by 5.7-cm long (axial direction) and are 1.3-cm thick. The top window is 0.64-cm thick and has a clear aperture that is 5.7-cm long and approximately 0.5-cm wide. Except for the areas near the windows, the walls are effusion-cooled. In addition, the sidewalls have a small gap between the window and the housing on the upstream side (see figure 3) that allows plenum air at the preheat temperature to pass over the inner window surface to keep the window clean and cool.

The pressure vessel is equipped with 6.4-cm thick fused silica windows that have a 15.2-cm diameter clear aperture. Six window ports are located circumferentially at 0° (top), 60°, 90°, 180°, 270°, and 315° around the housing. The inner window surfaces lie along a circle with diameter of 1.1-m. The vessel can support preheated temperatures up to 980 K at pressures up to 60 bar.

Optical Facility

A frequency-doubled Nd:YAG laser was used as the scattering source. The laser provided 532-nm light in 7-nsec pulses at a repetition rate of 10 Hz to the test rig. The incident laser beam traveled approximately 32 meters and was allowed to freely expand before focusing into the center of the vessel using a 50-mm-diameter, f = 1500 mm plano-convex lens. The beam entered vertically along the test rig's centerline, 55 mm downstream of the fuel injector exit plane. The laser energy at the focus was approximately 100 mJ/pulse.

Figure 5 illustrates the light collection optics. The Raman-scattered light originating approximately 4 mm above the test rig centerline is collected and collimated using a 100-mm-diameter, f = 350 mm plano-convex lens and is focused with an identical 100-mm lens onto a circular aperture (iris) before recollimating and refocusing the light using a pair of 50-mm, f = 200 mm, plano-convex lenses onto the 150-mm-wide entrance slit of the spectrometer. These paired lenses were selected to match the spectrometer's f-number. The overall system magnification of the optics matched with the test rig was 2.0. A 50-mm, O.D. = 6.0, 10-nm FWHM holographic notch filter centered at 532 nm, together with a 40-nm-wide band rejection filter centered at 530 nm were placed in the collimated path between the 50-mm lenses to reject unwanted Rayleigh and Mie laser scatter. The band rejection filter was added because the spectral envelope covered by the notch filter was insufficient to reject all laser scatter near 532 nm.

The Acton Spectra-Pro 300i used is an f/4 spectrometer with a focal length of 300 mm. Two gratings were used to spectrally resolve the Raman-scattered light and focus it onto the detector. We primarily used a 150 groove/mm grating blazed at 500 nm. We also occasionally used a grating with 600 groove/mm blazed at 300 nm. The 150-groove/mm grating provides the coverage to allow simultaneous recording of both anti-Stokes and Stokes lines.

The detector is a Princeton Instruments gated and intensified CCD camera having a detector array of 384×576 pixels on a 0.5-inch format chip. The spectrometer/camera combination provided a resolution of 0.471 nm/pixel for the 150-groove grating and 0.113 nm/pixel for the 600-groove grating. The laser Q-switch synchronously triggered the 50-ns gate.

The laser beam and collection optics are guided to their test rig target using traversing stages that are set up so that their movement is coordinated. Using the traverse system enables us to maintain position relative to the test rig, which grows downstream (shifts axially) as the inlet air temperature and pressure increase. The optics are physically decoupled from the test rig so that alignment is maintained. The rig grew twenty-one millimeters over the course of the test run.

The photograph reproduced in figure 6 depicts the Raman detection system set up adjacent to the test rig. Flow passes from left to right. Bellows and black tubing were used between optics to minimize stray light scatter into the detector. During the test, the entire detection system, including the spectrometer and camera was also covered with black cloth for the same reason.

Test Procedure

Data were collected at selected test points from approach to full power conditions using Jet-A fuel. Inlet temperatures ranged from 660 K to 750 K, with pressures from 13.8 bar to 55.2 bar, and equivalence ratios (ϕ) between 0.35 and 0.55.

Most of the Raman data sets were acquired using the 150-groove/mm grating and by averaging 100 laser shots on the detector chip. Prior to obtaining the data corresponding to the test matrix, we acquired spectra in air while ramping up the inlet temperature to the first test point. These spectra were used to

determine the appropriate spectrally sensitive calibration factor, $C(\nu_S,\nu_{AS})$. C depends on the entire optical detection path, including the windows; therefore, C is specific to each experimental setup. C was determined in a manner similar to that described in the theory section of this paper.

In all cases, we obtained background spectra without the laser at each test point just prior to getting the Raman-scatter spectra. These background flame-emission spectra were subtracted on-chip during data acquisition.

Results and Discussion

Summary

The gas sample probes that are typically used to measure major combustion species (O_2, N_2, H_2O, CO_2, unburnt hydrocarbons) and to derive the combustion temperature and efficiency were unavailable due to their failure during earlier tests of the same hardware. Because this test was primarily a proof-of-concept experiment, lack of actual gas sample data for direct comparison, though disappointing, was not overly restrictive. We assumed that the averages we obtained 55 mm downstream of the injectors to be representative of the average post-combustion bulk temperature.

The graph of figure 7 summarizes the results obtained during this test using spontaneous Raman scattering. The graph plots the derived local Raman combustion temperatures and the theoretical temperatures based on the inlet conditions. The theoretical curve is calculated from the relation developed by Wey (2001) and used in the facility operations and data processing software. The relationship is

$$T_{flame}(^\circ K) = T_{inlet}(1-\phi(0.6104-0.2633\phi))+\phi(3023.23-924.51 \qquad (2)$$

and holds for all fuel-lean Jet-A/air flames with ϕ less than 0.7. The graph consists of three linear least-square fits to the data or theory. The short-dashed line with square symbols is the theoretical curve. The long-dashed line with circles is the Raman-derived temperature based on our original calibration; the solid line with triangles is the corrected curve. The motivation to correct is based on knowledge about mid-test changes in the experiment optics resulting in a change in the calibration constant as the test run proceeded. Sources of error related to the background and in determination of the appropriate AS/S area ratios were considered relatively minor. Facility issues developed over the course of the run, including broken windows and burning upstream (and outside) of the test article; we determined that these were not of a significant nature to affect the overall discrepancy between the Raman and theoretical temperatures.

Figure 8 shows a few of the initial calibration spectra obtained prior to combustion during the ramp-up in inlet temperature. The inlet temperature increases from bottom spectrum to top. Each spectrum was acquired in air at 20 bar. Dotted lines show the N_2 anti-Stokes and Stokes peak locations at $\pm$ 2331 cm^{-1}. The room temperature spectrum shows no N_2 anti-Stokes peak, but the two elevated temperature spectra have small peaks just above the baseline. The areas above the baseline for each peak are used to calculate the ratios and determine the constant $C(\nu_S, \nu_{AS})$. As one can see, determining the anti-Stokes peak areas at "low" temperature is challenging, but not impossible.

Figure 9 plots the measured inlet temperatures against the Raman-derived temperature for the data obtained during temperature ramp-up. We determined the calibration factor for this particular optical setup to be 0.81. The data acquired using the 150- and 600 groove/mm gratings show good agreement with the ASCR facility-measured temperatures.

We believe this initial calibration is correct for two reasons. First, the agreement was good for both gratings. Secondly, points taken early in the run show virtually no differences with the theoretical reference curve. The departure from theoretical occurs abruptly and continues on from that point. The time of the change occurred immediately after an unplanned mid-test rig shutdown.

After the test, we saw that both combustor sidewall windows were abraded in places due to the heat of the flame. These areas had a sandblasted, frosty appearance. The collection window was cracked. Figure 10 shows a fragment of that window. The large outer shell window on the collection side was undamaged, but its counterpart on the opposite side was badly cracked. We also found the top casing window—the laser input window—broken and lying atop the combustor case. The retaining bracket that normally holds the window in place had become loose. Only a small piece of the window remained, roughly one-third its original size. Although some plenum air may have entered the combusting region through the top, there was no significant change in the measured inlet and exit parameters, suggesting no real effect on combustion temperatures.

The combustor sidewall window was coated with soot deposits, which can be seen in figure 10. It is possible that the unscheduled mid-test shutdown promoted soot deposition. We used a spectrophotometer to determine the transmission characteristics of the used window compared to an unused window. We found that the unused window has a very slight drop-off in transmittance of the AS line compared to the Stokes line, less than one percent. The used window showed a noticeable difference, however, decreasing by 8 per cent. This decrease is for a room temperature window. We do not know what the effect is at combustion temperatures, although there is little effect between 298 K and 873 K (Stagg and Charalampopoulos, 1993). We cannot say whether more soot was present on the window during the run. Additionally, the location on the used window that we scanned was moderately coated, and not in the heaviest location so that the effect would have been worse than the graph indicates. Soot may have been blown off during the post-combustion cool down period; if such is the case, then the decrease in transmission could have been well in excess of 10 percent. We believe the soot was the single largest factor in the discrepancy between our Raman results and the theoretical values.

Soot continues to be studied and modeled intensively because of the large roles it plays in combustion and emissions, in particular for radiative heat transfer inside the engine. Among these efforts is determining soot's optical properties—indices of refraction—to be able to characterize the spectral scatter, absorption, and extinction. Krishnan et al. (2000, 2001) reported values of refractive index functions for absorption and scattering as a function of wavelength. We find that the values of these functions change by a factor of from 1.2 to 1.7 for the wavelength regions of concern here.

We used two values for the calibration constant, $C(\nu_S, \nu_{AS})$. The value 0.81 was used for the points acquired before the unplanned shutdown; 1.32 was used for all points thereafter. This is an increase in the calibration constant by a factor of 1.6. We are confident that the adjustment makes sense in light of the window deposits. Another point validating the correction is that the single adjustment causes the Raman-generated temperatures (as seen in figure 7) to more closely match the theoretical temperatures. Since each curve is nonlinear in a different manner and completely independent, this strong correlation adds credibility to the correction.

Except for the discrepancy that we attribute to soot's effect on the calibration constant, we show very encouraging results for this first-ever application of spontaneous Raman scattering to measure temperature in a major production research facility.

Spectra Obtained During Combustion

We discuss in this section some details of the spectra obtained and describe the challenges we see in obtaining spectra that can be used to accurately measure combustion temperature. We would like particularly to achieve high-quality single-shot spectra so that we may begin to describe statistically similar turbulent combusting systems.

Figure 11 plots as a function of frequency shift a few spectra obtained during combustion. Figures 11(a)-11(c), plotted from high to low pressure, are Raman spectra. Figure 11(d) is a background emission spectrum obtained without the laser.

Figure 11(a) was acquired at a point with inlet temperature, pressure and flow rate of 717 K, 54 bar (800 psia), and 6.0 kg/s. The equivalence ratio is 0.35. The N_2 peaks for both the anti-Stokes and Stokes lines are distinct. Although both N_2 peaks are discernable and we were able to determine the AS/S ratio, this is not necessarily as clear in every case. For example, in figure 11(b), it is more difficult to distinguish the AS peak from the baseline. Though there is the obvious temperature effect, we believe that if we improve other factors in the experiment, we can increase the AS signal, thereby enhancing our ability to determine the AS/S ratios. There are two areas in particular that we feel should be improved, signal filtering and accounting for background emissions.

The notch and band rejection filters each has a lower transmission for the AS band than for the Stokes band of roughly 10-12 percent. By using both filters we compound the discrepancy by rejecting nearly 50 percent of the AS signal compared to between 25-30 percent if only one filter is used. Even though we account for the difference in spectral response when we determine $C(\nu_S, \nu_{AS})$, a higher AS transmission would enhance our signal and possibly make determining the peak area ratios easier to evaluate. Thus, there is room for significant improvement in this area. Given the spectral width of the laser, the obvious options are to consider a notch filter with a wider rejection band and possibly a greater optical density within the rejection region. Alternately, we may also look for band rejection filters with more favorable spectral transmission.

Although figure 11(d) is representative of all background spectra taken, the background spectra vary significantly in shape and slope, so it is important to subtract the appropriate background signal. We were unable to take background data simultaneously with the Raman spectra, therefore it is possible that the background emission that occurred when the Raman spectrum was obtained is somewhat different than the background spectra used, even though the inlet condition was the same. This is obviously the case, for example, when comparing figures 11(c) and 11(d), which were taken at the same inlet conditions. The Raman spectrum clearly has a shape that is consistent with the emission spectra. Thus, for this case the background level during data acquisition was somewhat greater than when the background file was obtained. Differences in background are reflected in the other spectra of figure 11 as well, as evidenced by the different slopes and shapes of the baselines.

For determining peak areas, we are interested in the area above the baseline. However, some error may be introduced when it is difficult to determine the actual slope or curvature of the baseline, especially if the peak in question is not very high above that baseline. In future work we will pursue ways to obtain the baseline much more proximate in time with Raman scattering data. Such “simultaneous” data acquisition will be important as well, as we strive to obtain high-quality single-shot spectra.

Our greatest challenge in accurately measuring temperature perhaps will be in compensating for the effect of soot on the calibration factor. In order to address possible changes to the wavelength-dependent calibration factor, we plan to periodically monitor the system’s spectral response using a calibration lamp. Comparison to a benchmark taken before the test will enable us to determine and apply corrections as needed. Together with better filtering and better background compensation, these considerations will also be needed for any future developments to obtain reliable single-shot spectra.

Conclusion

We have successfully demonstrated the practical application of the spontaneous Raman anti-Stokes/Stokes peak ratio method to measure combustion temperature in a kerosene-fueled, aviation gas turbine combustor. This work marks the first-ever use in a high-pressure, continuous flow facility using real com-

bustor hardware. A discrepancy between the Raman-derived temperatures and the theoretical calculation is attributed to the presence of soot on the windows and/or in the flame itself. With small modification to our procedure, we believe we can compensate for the effect of soot.

References

Eckbreth, A.C. (1988) *Laser diagnostics for combustion temperature and species*, Abacus Press, Cambridge.

Hicks, Y.R., Locke, R.J., and Anderson, R.C. (2000) Optical measurement and visualization in high-pressure, high-temperature, aviation gas turbine combustors, in Optical Diagnostics for Industrial Applications, Halliwell, N. A. (Ed.), Proceedings of SPIE Vol. 4076, pp. 66–77.

Karpetis, A.N. and Gomez, A. (1996) Temperature measurements in spray flames by spontaneous Raman Scattering, *Optics Letters*, Volume 21, Number 10, pp.704–706.

Krishnan, S.S., Lin, K.-C., and Faeth, G.M.(2000) Optical properties in the visible of overfire soot in large buoyant turbulent diffusion flames, *Journal of Heat Transfer*, Volume 122, pp. 517–524.

Krishnan, S.S., Lin, K.-C., and Faeth, G.M.(2001) Extinction and scattering properties of soot emitted from buoyant turbulent diffusion flames, *Journal of Heat Transfer*, Volume 123, pp. 331–339.

Laurendeau, N.M (1988) Temperature measurements by light-scattering methods, *Prog. Energy Combust.Sci*., Volume 14, pp.147–170.

Lederman, S. (1977) The use of laser raman diagnostics in flow fields and combustion, *Prog. Energy Combust. Sci.*, Volume 3, pp.1–34.

Locke, R.J., Hicks, Y. R., Degroot, W.A., and Anderson, R.C. (2001) Non-intrusive, laser-based imaging of jet-A fuel injection and combustion species in high pressure, subsonic flows, 37th JANNAF Combustion, Propulsion Systems Hazards, and Airbreathing Propulsion Subcommittees Joint Meeting. Monterey, CA, November 2000. NASA TM—2001-211113, August.

Mansour, A., Laing, P., Harvey, R., and Tacina, R. (2001) "Integrated Fuel Injection and Mixing System with Impingement Cooling Face", Patent pending.

Stagg, B.J. and Charalampopoulos, T.T. (1993) Refractive indices of pyrolytic graphite, amorphous carbon, and flame soot in the temperature range 25° to 600°C, *Combustion and Flame*, Volume 94, pp.381–396.

Tacina, R., C. Wey, P. Laing, and A. Mansour (2002) Sector tests of a low-NOx, lean-direct-injection, multipoint integrated module combustor concept, GT-2002-30089, proceedings of ASME Turbo Expo 2002, Amsterdam, The Netherlands, June 2002.

Wey, C. (2001) Personal communication.

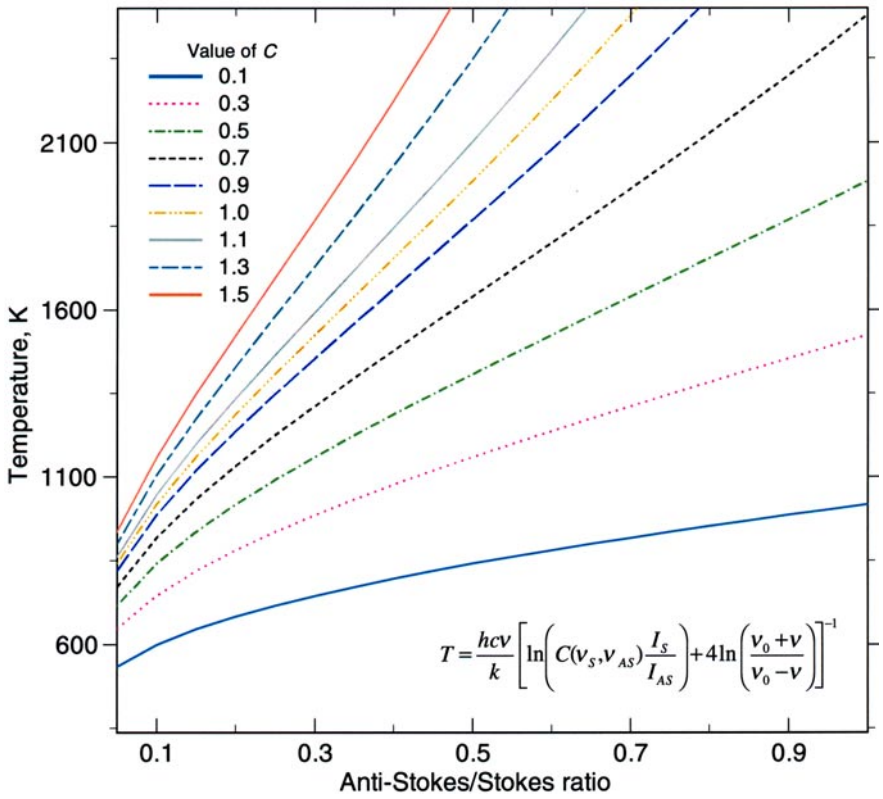

Figure 1.—Theoretical curves of the temperature using the Anti-Stokes/Stokes development of equation 1.

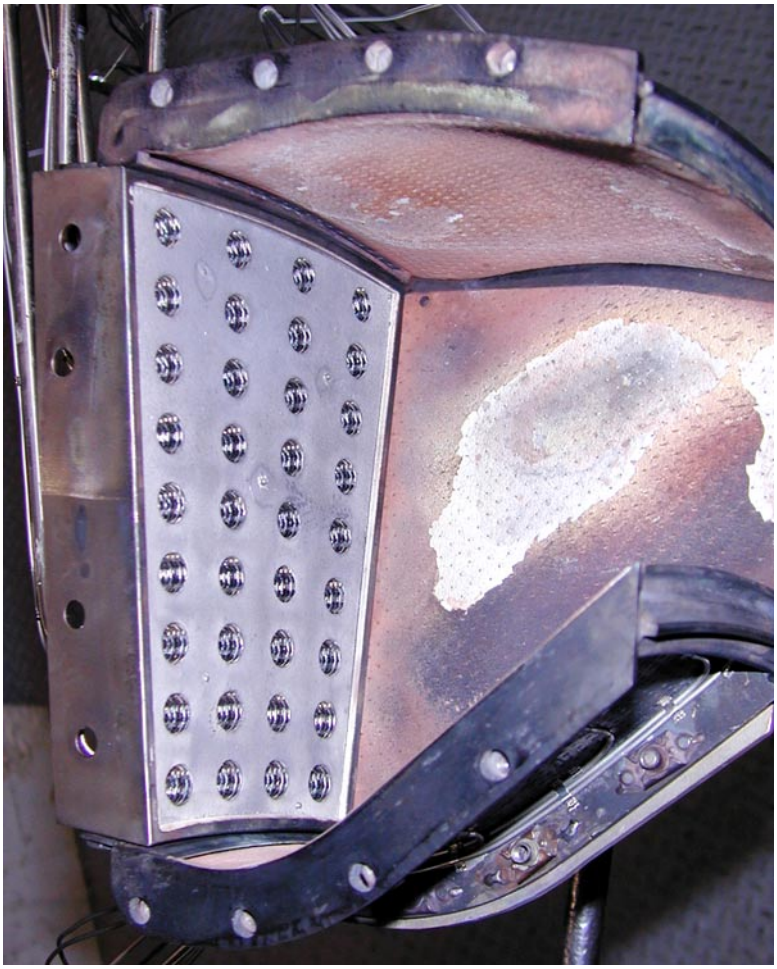

Figure 2.—Photograph showing the NASA-concept multipoint LDI injector used, the port combustor sidewall, and the top and bottom liners. Flow is from left to right.

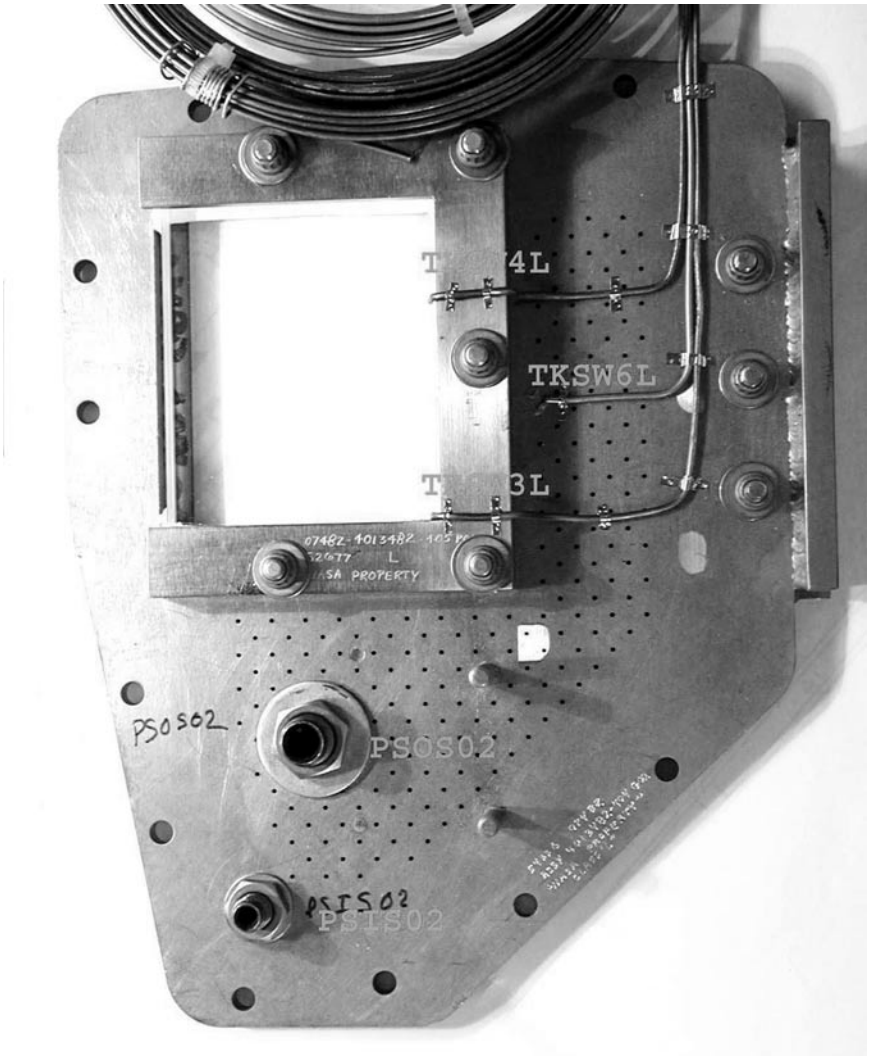

Figure 3.—The exterior side of the starboard combustor sidewall window housing, instrumented with thermocouples. Flow passes from left to right.

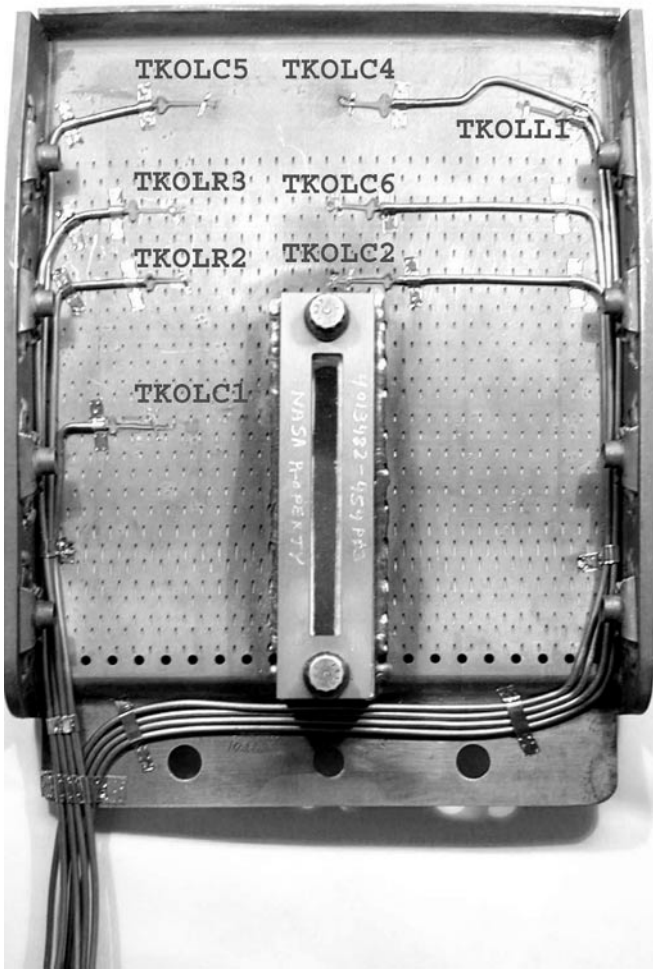

Figure 4.—The combustor top wall (liner) equipped to hold the top window. Flow travels from bottom to top.

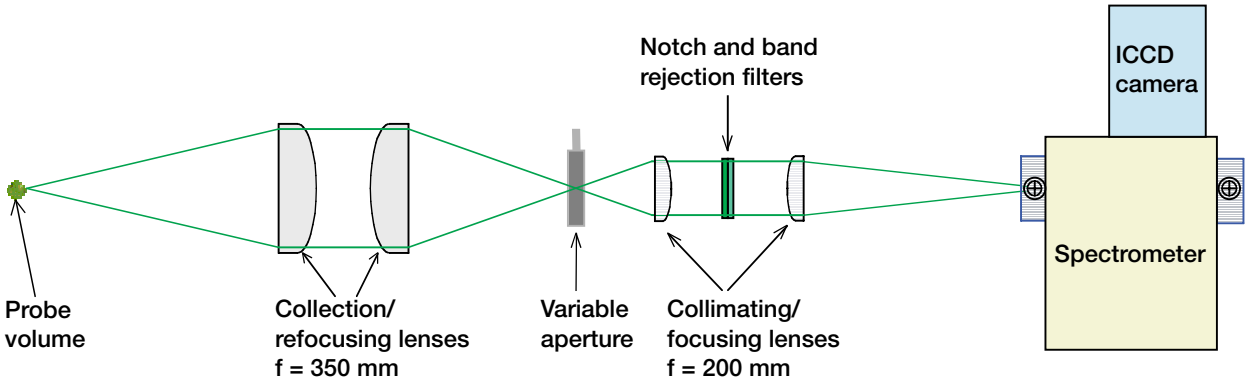

Figure 5.—Schematic drawing of the Raman light-collection system.

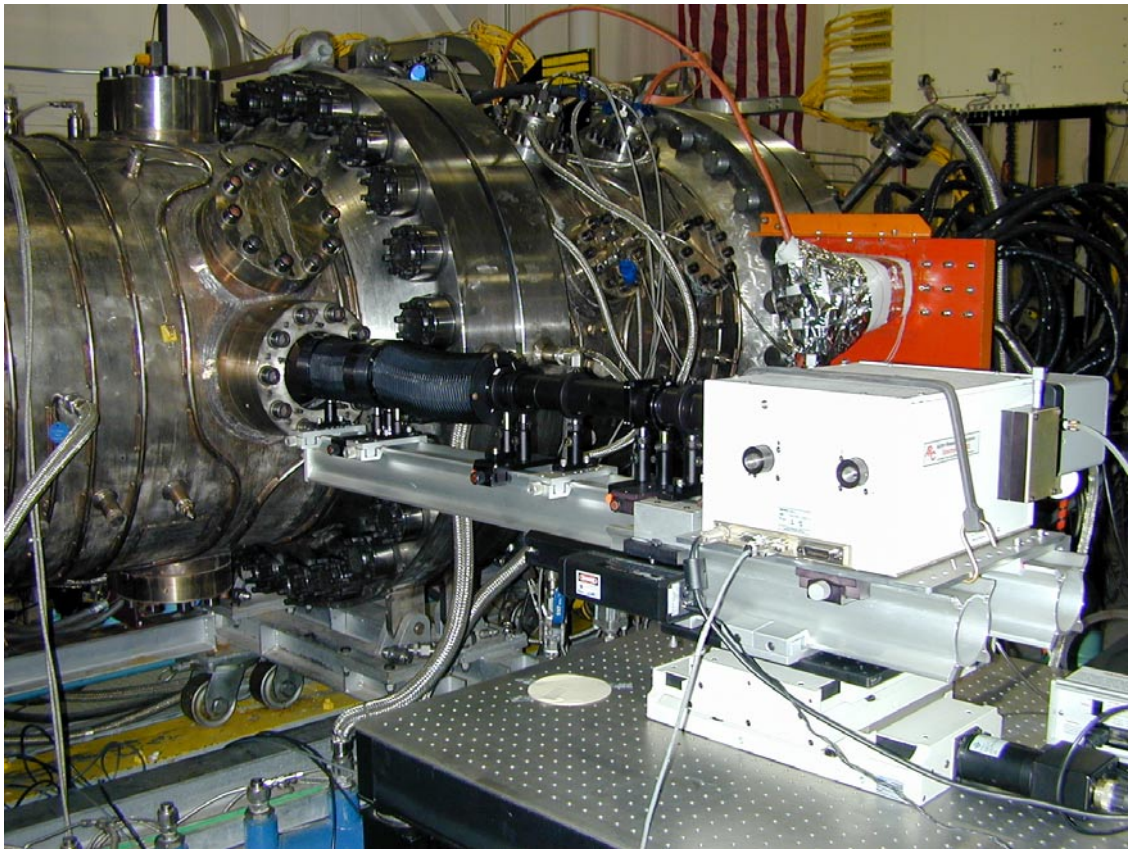

Figure 6.—The Raman setup in the ASCR test facility showing the receiving optics train, spectrometer and camera relative to the sector outer collection window. Flow passes from left to right.

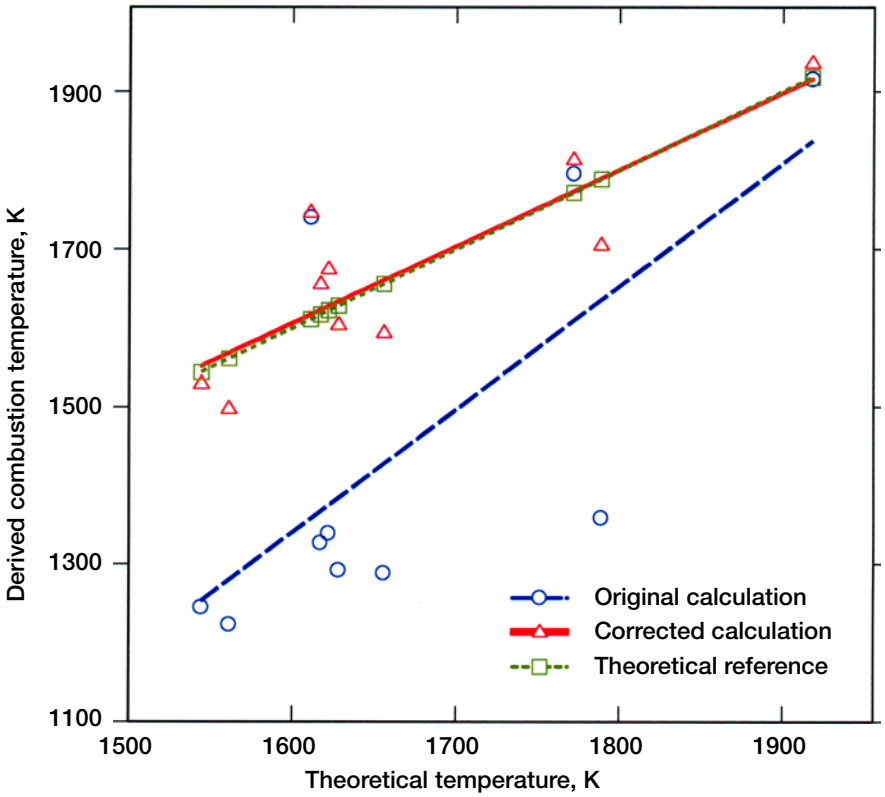

Figure 7.—Comparison of the Raman-derived combustion temperature with the theoretical values based on inlet conditions.

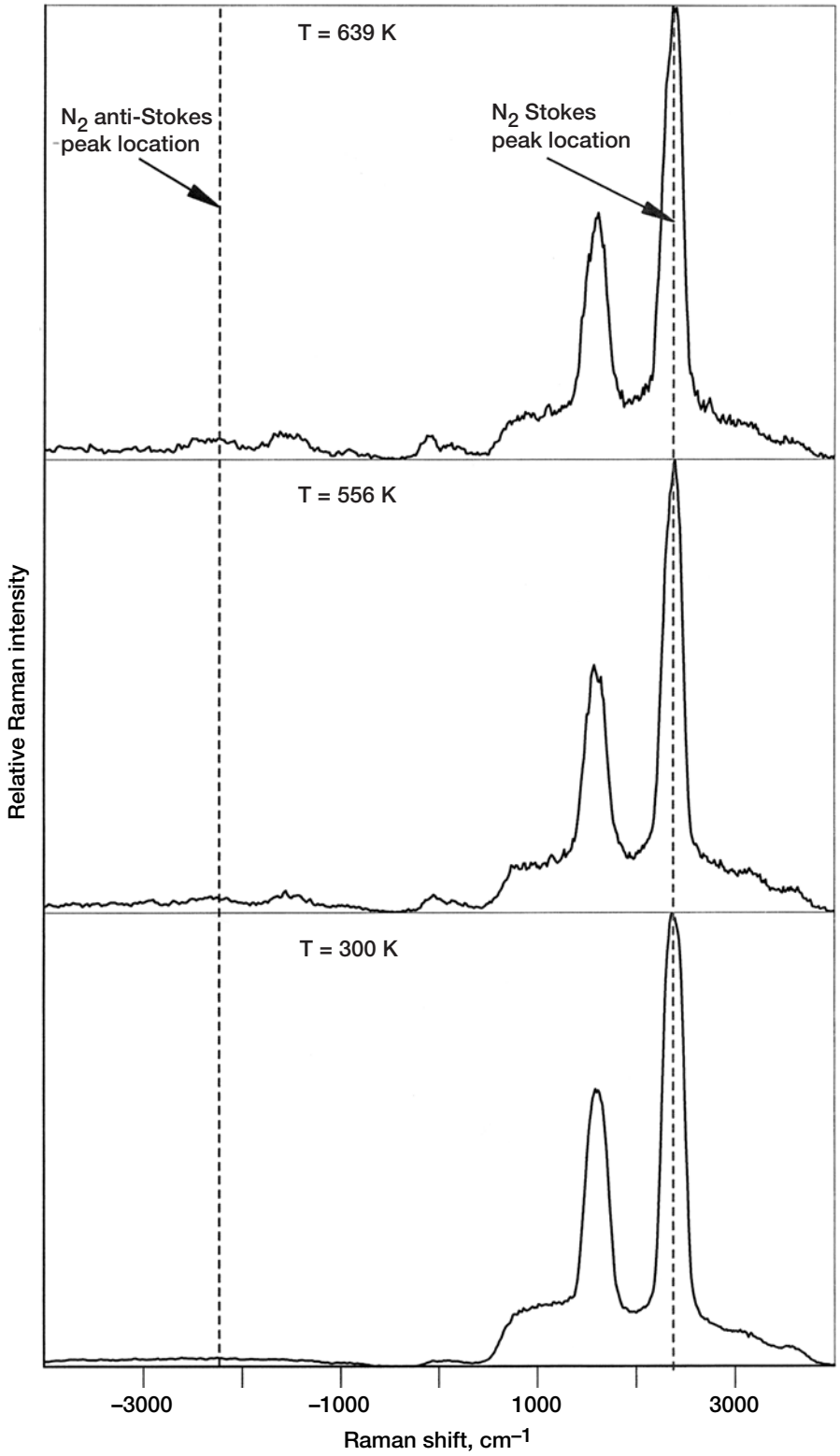

Figure 8.—Raman spectra for three preheat air-only cases. The rig pressure is 20 bar. Temperatures are noted on each graph.

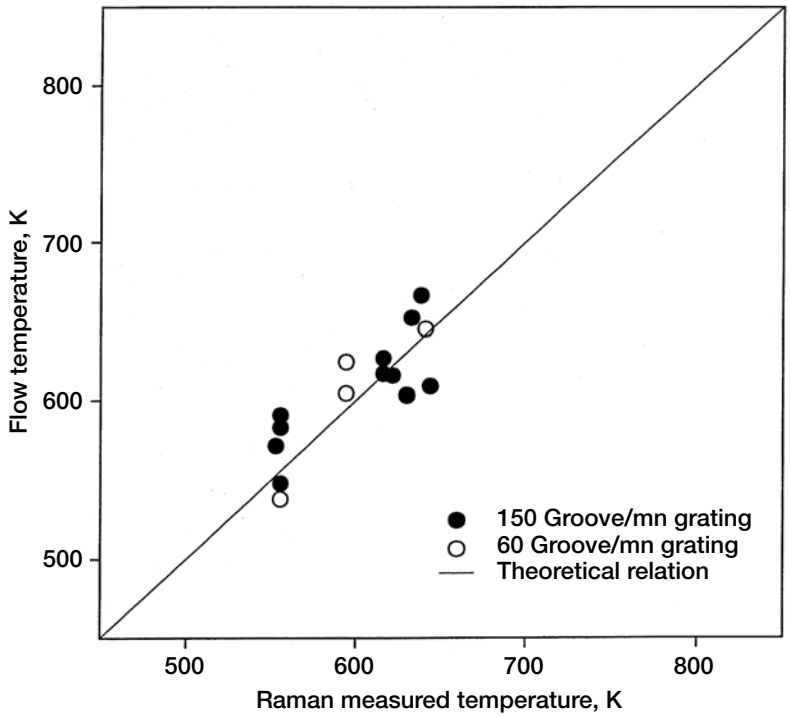

Figure 9.—Comparison of actual flow temperatures and Raman-measured temperatures for each spectrometer grating.

Figure 10.—Part of the inner side window on the detector side. The deposits have different spectral absorption characteristics at the N_2 Stokes and anti-Stokes lines.

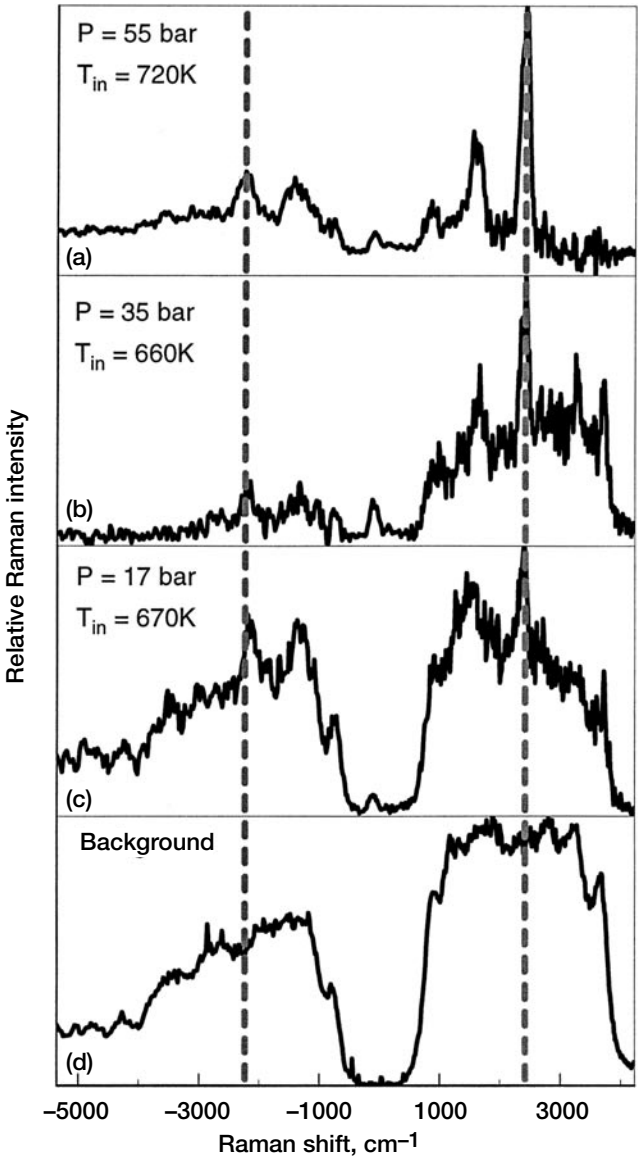

Figure 11.—Four spectra obtained during combustion. The values of P (bar), T (K), equivalence ratio, and airflow rate (kg/s) of the three Raman spectra are (a) 55 / 720 / 0.35 / 6; (b) 34 / 660 / 0.41 / 3.9; (c) 17 / 670 / 0.55 / 1.5. (d) is a background emission spectrum obtained at the conditions of (c).

REPORT DOCUMENTATION PAGE

Form Approved
OMB No. 0704-0188

1. AGENCY USE ONLY (*Leave blank*)	2. REPORT DATE	3. REPORT TYPE AND DATES COVERED
	May 2002	Technical Memorandum

4. TITLE AND SUBTITLE

Combustion Temperature Measurement by Spontaneous Raman Scattering in a Jet-A Fueled Gas Turbine Combustor Sector

5. FUNDING NUMBERS

WU–714–02–40–00

6. AUTHOR(S)

Yolanda R. Hicks, Wilhelmus A. De Groot, Randy J. Locke, and Robert C. Anderson

7. PERFORMING ORGANIZATION NAME(S) AND ADDRESS(ES)

National Aeronautics and Space Administration
John H. Glenn Research Center at Lewis Field
Cleveland, Ohio 44135–3191

8. PERFORMING ORGANIZATION REPORT NUMBER

E–13373

9. SPONSORING/MONITORING AGENCY NAME(S) AND ADDRESS(ES)

National Aeronautics and Space Administration
Washington, DC 20546–0001

10. SPONSORING/MONITORING AGENCY REPORT NUMBER

NASA TM—2002-211588

11. SUPPLEMENTARY NOTES

Yolanda R. Hicks and Robert C. Anderson, NASA Glenn Research Center; Wilhelmus A. De Groot, Silicon Light Machines, Sunnyvale, California 94089; and Randy J. Locke, QSS Group, Inc., Cleveland, Ohio 44135. Responsible person, Yolanda R. Hicks, organization code 5830, 216–433–3410.

12a. DISTRIBUTION/AVAILABILITY STATEMENT

Unclassified - Unlimited
Subject Categories: 01, 09, and 35 Distribution: Nonstandard

Available electronically at http://gltrs.grc.nasa.gov/GLTRS

This publication is available from the NASA Center for AeroSpace Information, 301–621–0390.

12b. DISTRIBUTION CODE

13. ABSTRACT ***(Maximum 200 words)***

Spontaneous vibrational Raman scattering was used to measure temperature in an aviation combustor sector burning jet fuel. The inlet temperature ranged from 670 K (750 °F) to 756 K (900 °F) and pressures from 13 to 55 bar. With the exception of a discrepancy that we attribute to soot, good agreement was seen between the Raman-derived temperatures and the theoretical temperatures calculated from the inlet conditions. The technique used to obtain the temperature uses the relationship between the N_2 anti-Stokes and Stokes signals, within a given Raman spectrum. The test was performed using a NASA-concept fuel injector and Jet-A fuel over a range of fuel/air ratios. This work represents the first such measurements in a high-pressure, research aero-combustor facility.

14. SUBJECT TERMS

Raman spectroscopy; Combustion temperature; Optical diagnostics; High-pressure combustion

15. NUMBER OF PAGES

23

16. PRICE CODE

17. SECURITY CLASSIFICATION OF REPORT	18. SECURITY CLASSIFICATION OF THIS PAGE	19. SECURITY CLASSIFICATION OF ABSTRACT	20. LIMITATION OF ABSTRACT
Unclassified	Unclassified	Unclassified	